[AMERICAN JOURNAL OF SCIENCE, SCHAIRER VOL. 267-A, 1969, P. 209-232]

SYNTHESIS AND STABILITY OF Ti-ANDRADITE

H. G. HUCKENHOLZ*

Geophysical Laboratory, Carnegie Institution of Washington, Washington, D.C. 20008

ABSTRACT. Chemical analyses of Ti-rich grandites from magmatic and metamorphic rocks plot (molecular norm) in the enstatite ($MgO \cdot SiO_2$)–wollastonite ($CaO \cdot SiO_2$)–hematite (Fe_2O_3)–perovskite ($CaO \cdot TiO_2$) system on or below the plane wollastonite–hematite–perovskite and close to the join andradite ($3CaO \cdot Fe_2O_3 \cdot 3SiO_2$)–Ti-garnet ($3CaO \cdot Fe_2O_3 \cdot 3TiO_2$). The phase relationships in the plane wollastonite–hematite–perovskite bear directly on the formation of andradite and its Ti-bearing varieties.

A series of compositions were studied in this plane and along the join andradite ($3CaO \cdot Fe_2O_3 \cdot 3SiO_2$)–Ti-garnet ($3CaO \cdot Fe_2O_3 \cdot 3TiO_2$) by means of quenching experiments at temperatures between 1000° and 1400°C and at 1 atm pressure. Stable phases are garnet solid solution (ss), pseudowollastonite, hematite, and perovskite solid solution. $Garnet_{ss}$ appear on the liquidus between compositions of $andr_{86}Ti\text{-}gar_{14}$ and $andr_{71}Ti\text{-}gar_{29}$. $Garnet_{ss}$ + liquid react to $perovskite_{ss}$ + liquid at compositions of $andr_{70}Ti\text{-}gar_{30}$ to $andr_{53}Ti\text{-}gar_{47}$ and at a temperature of 1315 ± 2°C. Garnet composition $andr_{52}Ti\text{-}gar_{48}$ melts incongruently to $perovskite_{ss}$ + liquid at 1315 ± 2°C. A quaternary univariant line with $garnet_{ss}$, $perovskite_{ss}$, hematite, and liquid in equilibrium pierces the join andradite–Ti-garnet at a composition of $andr_{45}Ti\text{-}gar_{55}$ and at a temperature of 1310 ± 2°C. The maximum degree of solid solution of $3CaO \cdot Fe_2O_3 \cdot 3TiO_2$ in the stable garnet is 54.5 percent by weight at 1137°C. Above this temperature andradite is not stable as a single phase, and the stability field of $garnet_{ss}$ diminishes to compositions between $andr_{80}Ti\text{-}gar_{20}$ and $andr_{45}Ti\text{-}gar_{55}$. The cell parameter of andradite (12.053 ± 0.003 Å) increases with solid solution at the rate of 0.038 ± 0.002 Å and 0.040 ± 0.002 Å, respectively, for 10 wt percent and 10 mole percent Ti-garnet.

Additional runs were carried out along the join diopside ($CaO \cdot MgO \cdot SiO_2$)–titanium ferri-Tschermak's molecule ($CaO \cdot TiO_2 \cdot Fe_2O_3$) within the enstatite–wollastonite–hematite–perovskite system. Stable phases are clinopyroxene solid solution, garnet solid solution, hematite, perovskite solid solution, and magnetite solid solution. The solid solution of the titanium ferri-Tschermak's molecule in the diopside is less than 5 percent by weight. Ferri-diopside containing enstatite components and Ti-andradite occur in polyphase assemblages at solidus temperatures.

INTRODUCTION

Andradite, $Ca_3Fe_2^{3+}Si_3O_{12}$, and its titanium-rich varieties, melanite, schorlomite, and iiaavarite, are common garnets in alkaline igneous rocks and in thermally metamorphosed, impure limestone and skarn deposits. The origin of Ti-bearing andradites has been the subject of much discussion because the structural positions of Ti and its valency states remain problematical. Zedlitz (1933) suggested that a part of Ti is present in the trivalent state, but optical absorption spectra of a melanite specimen from San Benito County, California, obtained by Manning (1967) do not appear to prove adequately this assumption. Suitable ion distribution may be achieved in Ti-rich andradites by substituting Ti^{4+} for Fe^{3+} and Si. Infrared spectra of titaniferous garnets (Tarte, 1960) and the synthesis of germanate, rare-earth iron, and rare-earth gallium garnets (Espinosa, 1964; Ito and Frondel, 1967; Geller, 1967) have demonstrated that Ti^{4+} prefers the six-fold position in the garnet structure but may also enter a four-fold position. Most analyses of Ti-rich grandite garnets show an excess of tetravalent and divalent cations but a deficiency of the

* Present address: Mineralogisch-Petrographisches Institut der Universität zu München, München, Germany.

trivalent group. This fact indicates that $2R^{3+}$ cations (Fe^{3+}, Al) may also be replaced by $R^{4+}R^{2+}$ (Ti^{4+} and Mg,Fe^{2+},Mn), as demonstrated by Geller, Miller, and Treuting (1960) for germanate garnets having $Ti^{4+}Mg$, $Ti^{4+}Ni$, and $Ti^{4+}Co$ in place of $2R^{3+}$. Some of the Ti-garnet analyses report alkalies, and if they are not attributable to impurities, a minor substitution of $NaTi^{4+}$ for $CaFe^{3+}$ may be possible too.

In dealing with garnet analyses, one has to keep in mind the great separatory and analytical difficulties, particularly if minute inclusions are involved and if the ferric iron content is high compared with the ferrous iron. However, chemical analyses of Ti-garnets may be balanced ionically within the limit of error. (In some older analyses which show an excess of R^{+4} cations, a conversion of Ti^{4+} to Ti^{3+} would have been necessary but a change of Fe^{3+} to Fe^{2+} would have the same balancing effect. Such analyses have been neglected here). The generalized formula of Ti-rich grandite garnets as considered in this study may be expressed on the basis of 24 oxygens as

$$(Ca,Na,Fe^{2+},Mg)_6(Fe^{3+},Ti^{4+},Al,Mg,Fe^{2+},Mn)_4\ (Si,Al,Fe^{3+},Ti^{4+})_6\ O_{24}.$$

As a first approximation, reliable chemical analyses of Ti-rich grandites from both igneous (49) and metamorphic rocks (12) plot (molecular norm) in the enstatite ($MgO\cdot SiO_2$)–wollastonite ($CaO\cdot SiO_2$)–hematite (Fe_2O_3)–perovskite ($CaO\cdot TiO_2$) system on or below the plane wollastonite–hematite–perovskite (fig. 1) and close to the join andradite ($3CaO\cdot Fe_2O_3\cdot 3SiO_2$)–Ti-garnet ($3CaO\cdot Fe_2O_3\cdot 3TiO_2$), correcting for a minor content of alkalies as a $Na_2O\cdot CaO\cdot 2TiO_2\cdot 3SiO_2$ component. Hypothetical garnet components may be calculated on the basis of enstatite, wollastonite, hematite and perovskite. After deduction of $Na_2O\cdot CaO\cdot 2TiO_2\cdot 3SiO_2$ (Na-melanite) the remaining sum of wo + en + fs + pv is equal to or larger than 3(hem + c) in acceptable analyses and may be expressed as a mixture of

1 en + 2 wo + 1 pv = Mg-melanite ($3CaO\cdot MgO\cdot TiO_2\cdot 3SiO_2$)
1 fs + 2 wo + 1 pv = Fe-melanite ($3CaO\cdot FeO\cdot TiO_2\cdot 3SiO_2$)

if wo + en + fs + pv > 3(hem + c). If wo + en + fs + pv = 3(hem + c) the following additional components may be formed:

3 pv + 1 hem = melanite ($3CaO\cdot Fe_2O_3\cdot 3TiO_2$)
3 en + 1 hem = khoharite ($3MgO\cdot Fe_2O_3\cdot 3SiO_2$)
3 fs + 1 hem = skiagite ($3FeO\cdot Fe_2O_3\cdot 3SiO_2$)
3 wo + 1 hem = andradite ($3CaO\cdot Fe_2O_3\cdot 3SiO_2$) } grandite
3 wo + 1 c = grossularite ($3CaO\cdot Al_2O_3\cdot 3SiO_2$) }

Ti-rich grandites from the Kaiserstuhl volcanic area, Germany, and from Magnet Cove, Arkansas, have the composition (mole percent) given in table 1.

THE JOIN ANDRADITE—Ti-GARNET

In order to obtain information about the nature of the incorporation of titanium (calculated as tetravalent) in andradite, a series of nine-

teen compositions in the plane wollastonite–perovskite–hematite was prepared along the join andradite–Ti-garnet and for four additional compositions in this plane. DeVries, Roy, and Osborn (1956) examined the join wollastonite–perovskite at 1 atm. Ito and Frondel (1967) studied parts of the join andradite–Ti-garnet from $andr_{100}$Ti-gar_0 to $andr_{31}$ Ti-

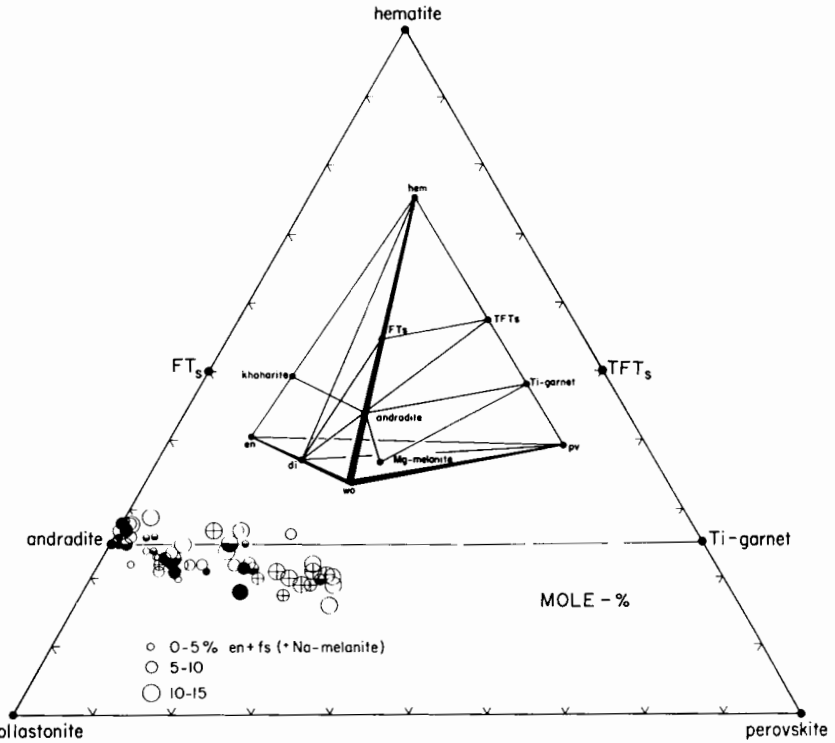

Fig. 1. The quaternary system en-wo-pv-hem, which includes the join wollastonite-perovskite-hematite with a plot of analyses of Ti-bearing garnets from metamorphic (solid circles), alkaline plutonic (open circles), alkaline volcanic (half shaded circles, and alkaline hypabyssal rocks (circles with crosses). Abbreviations and compositions of phases encountered: hem, Fe_2O_3; TFT_s $CaO \cdot Fe_2O_3 \cdot TiO_2$; FT_s, $CaO \cdot Fe_2O_3 \cdot SiO_2$; pv, $CaO \cdot TiO_2$; wo, $CaO \cdot SiO_2$; di, $CaO \cdot MgO \cdot 2SiO_2$; en, $MgO \cdot SiO_2$; khoharite, $3MgO \cdot Fe_2O_3 \cdot 3SiO_2$; andradite, $3CaO \cdot Fe_2O_3 \cdot 3SiO_2$; Ti-garnet, $3CaO \cdot Fe_2O_3 \cdot 3TiO_2$; and Mg-melanite, $3CaO \cdot MgO \cdot TiO_2 \cdot 3SiO_2$; as well as fs, $FeO \cdot SiO_2$ and Na-melanite, $Na_2O \cdot CaO \cdot 2TiO_2 \cdot 3SiO_2$. Data were taken from Brauns, 1922, p. 126, nos. VI, VII; Carpanese, 1932; Clark, 1957; Deer, *in* Deer, Howie, and Zussman, 1962, v. 1, p. 91, table 15, no. 8; Erickson and Blade, 1963, p. 74, table 58; Genth, 1890; Gossner, 1931, p. 228; Gossner and Reindl, 1934, p. 161; Hackmann, 1900, p. 11, no. 1; King, 1949, p. 43, no. B; König, 1886, p. 335, nos. 1*, 2*; Knop, 1877, p. 63, nos. C*, D*; Kunitz, 1936, p. 395, table 11, nos. 1, 2, 3, 4, 5; Larsen and Jenks, 1942, p. 54, table 25*; Majer, 1954; Miyashiro, 1959, p. 171, table 1; Piners, 1894, p. 481, 490, 492, 493; Sanero, 1935; Seebach, 1906, p. 778, table IV, no. 1; Subramanim, 1956; Sobolev, 1964, nos. 983, 984*, 985, 987, 989*, 990*, 991, 992, 993, 994, 995, 997, 999, 1000, 1001, 1002, 1003, 1005, 1009, 1012, 1013, 1014, 1015, 1016, 1021, 1027, 1028; Washington, 1920, p. 41; Zedlitz, 1933, p. 228, table 2; 1933, p. 71, table 2, p. 73, table 4*.

* Total Fe reported as Fe_2O_3, corrected for FeO in this paper to fit the garnet formula.

gar_{69} at 1050°C and 1 atm, using gel techniques. The latter authors reported a maximum heating time of 20 hours for the formation of a garnet solid solution, far short of the time required to attain equilibrium in the present study, in which glasses and crystallized glasses were used. At least 50 days at 1050°C are necessary with 10 thorough grindings during the crystallizing period for a complete solution of all metastably formed wollastonite in the $garnet_{88}$, even when the starting material is a very fine powdered glass (fig. 2). No wollastonite and pseudowollastonite (or traces only) were formed from a starting material that was prepared in this way when treated under subsolidus conditions at temperatures between 1000°C and 1268°C. The data in the present investigation were obtained by quenching experiments (Shepherd and Rankin, 1909), in which mixtures had been held between 1000° and 1400°C at 1 atm pressure. Results are presented in tables 2 and 3, as well as in a T-X diagram (fig. 3) and in seven critical and unique isothermal sections of the wollastonite–hematite–perovskite plane. Ubiquitous ferrous iron was analyzed in runs that were treated at temperatures of 1100° and 1250°C and in starting material that was quenched from 1500°C. Data are given in table 6 and figure 5.

TABLE 1

Chemical composition, molecular norm, and hypothetical garnet components in mole percent from two Ti-bearing garnets

	1	2		1	2
Chemical composition			Garnet components		
SiO_2	27.94	27.89	Na-melanite	3.4	...
TiO_2	12.10	15.51	Mg-melanite	3.6	16.0
Al_2O_3	5.17	2.12	Fe-melanite	12.4	15.3
Fe_2O_3	17.47	18.32	Melanite	16.9	22.7
FeO	3.26	2.91	Khoharite	...	...
MnO	0.27	0.57	Skiagite	3.6	3.1
MgO	0.31	1.22	Andradite	36.0	32.5
CaO	31.90	31.79	Grossularite	24.1	10.4
Na_2O	0.52	...			
K_2O	0.14	...			
H_2O	0.59	...	Molecular norm		
Totals	99.93	100.33	Na-melanite	3.4	...
			hem + c	19.2	17.3
			pv	17.6	24.8
			en	0.9	4.0
			fs	6.1	6.1
			wo	52.8	47.8

1. Melanite from phonolite, Oberrotweil, Kaiserstuhl volcanic area, Germany (Zedlitz, 1933).

2. Melanite from biotite-garnet ijolite, alkaline igneous complex, Magnet Cove, Arkansas (Erickson and Blade, 1963).

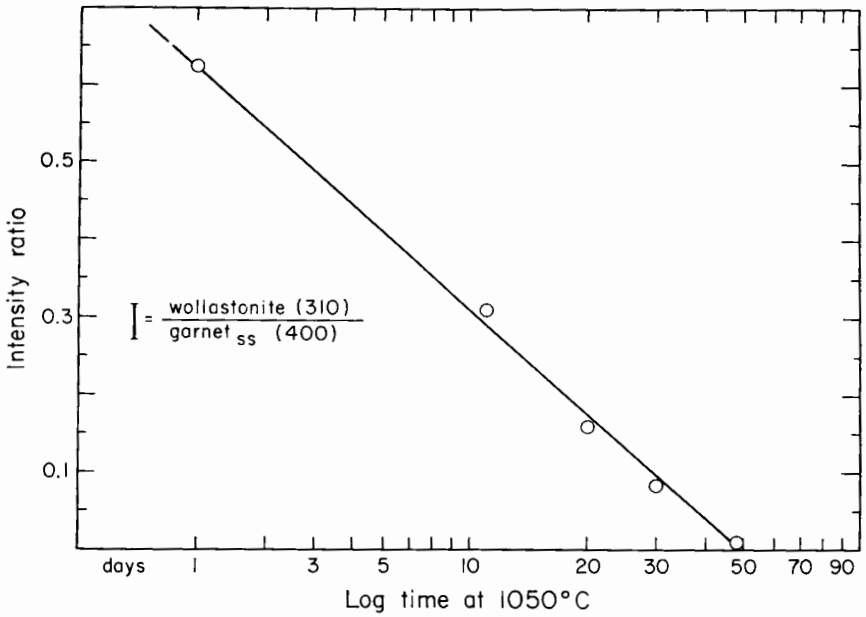

Fig. 2. The solution of metastable wollastonite in the garnet solid solution of $andr_{90}Ti\text{-}gar_{10}$ as a function of time based on relative intensities of the (310) and (400) reflections respectively.

The stable phases crystallizing on the join andradite–Ti-garnet (fig. 3) are garnet solid solution (gar_{ss}), pseudowollastonite (pwo), hematite (hem), and perovskite solid solution (pv_{ss}). Garnet solid solutions having compositions that correspond to the join andradite–Ti-garnet, perovskite solid solution, pseudowollastonite, hematite and, above 1268°C, even the liquid are on or very close to the ternary join wo-pv-hem. Fine-grained, mosaic intergrowths with an average grain size of 5 to 10 microns are typical for garnet solid solutions that crystallize on the joins. When quenched from temperatures close to the beginning of melting garnet crystals of about 25 to 40 microns are obtained. The color changes from an almost colorless andradite through a light yellow to a dark yellow brown at $andr_{45}$ $Ti\text{-}gar_{55}$. $Garnet_{ss}$ occuring on the liquidus are isometric and poorly facetted in most cases. $Perovskite_{ss}$ crystallizes as euhedral crystals of 2 to 5 microns, which coalesce very often to chains and clouds, and pseudowollastonite forms stout prisms in the glass. Polyphase assemblages consist of fine-grained intergrowths of the phases present. In these particular cases perovskite occurs as rounded grains having weak birefringence. Hematite forms irregular plates and patches. Pseudowollastonite is embedded in a fine mosaic of $garnet_{ss}$.

The maximum degree of solid solution of $3CaO \cdot Fe_2O_3 \cdot 3TiO_2$ in the stable garnet is 54.5 percent by weight at a temperature of 1137°C. A composition of $3CaO \cdot Fe_2O_3 \cdot 1.5TiO_2 \cdot 1.5SiO_2$ is obtained close to 1000°C.

TABLE 2

Quenching results for compositions along the join andradite—Ti-garnet

Composition	Starting material	T, °C	Time	Products	Remarks
$andr_{100}Ti\text{-}gar_0$	xtl	1345	2 hr	glass	
	xtl	1340	2 hr	glass + pwo	pwo in moderate amounts
	glass	1295	24 hr	glass + pwo	
	xtl	1295	24 hr	glass + pwo	glass in small amounts
	xtl	1290	24 hr	pwo + hem	
	xtl	1160	28 days	pwo + hem	traces of gar_{ss}
	glass	1160	28 days	pwo + hem	
	xtl	1155	28 days	pwo + hem + gar_{ss}	gar_{ss} in traces
	glass	1155	28 days	pwo + hem + gar_{ss}	gar_{ss} in small amounts
	xtl	1150	14 days	pwo + hem + gar_{ss}	
	glass	1150	14 days	pwo + hem + gar_{ss}	
	xtl	1140	14 days	pwo + hem + gar_{ss}	traces of wo
	glass	1140	14 days	pwo + hem + gar_{ss}	hem in traces
	xtl	1135	14 days	andr	traces of wo and hem
	glass	1135	14 days	andr	traces of wo and hem
	glass	1135	56 days	andr	
$andr_{95}Ti\text{-}gar_5$	glass	1325	2 hr	glass	
	glass	1320	2 hr	glass + pwo	pwo in small amounts
	glass	1280	24 hr	glass + pwo	
	glass	1275	7 days	glass + pwo + hem	hem in small amounts
	xtl	1270	3 days	glass + pwo + hem	
	xtl	1265	3 days	pwo + hem + gar_{ss}	
	glass	1175	14 days	gar_{ss}	traces of pwo + hem
	xtl	1150	20 days	gar_{ss}	
$andr_{90}Ti\text{-}gar_{10}$	glass	1300	2 hr	glass	
	glass	1295	20 hr	glass + pwo	pwo in small amounts
	glass	1275	7 days	glass + pwo	
	xtl	1275	7 days	glass + pwo	traces of hem
	xtl	1270	3 days	glass + pwo + hem	
	glass	1265	3 days	pwo + hem + gar_{ss}	
	xtl	1225	3 days	pwo + hem + gar_{ss}	
	xtl	1200	7 days	gar_{ss}	traces of pwo + hem
	glass	1200	7 days	gar_{ss}	
$andr_{85}Ti\text{-}gar_{15}$	xtl	1290	2 hr	glass	
	xtl	1285	20 hr	glass + gar_{ss}	small amount of gar_{ss}
	xtl	1280	20 hr	glass + gar_{ss} + pwo	
	xtl	1265	3 days	gar_{ss} + pwo + hem	
$andr_{80}Ti\text{-}gar_{20}$	glass	1290	2 hr	glass	
	glass	1285	20 hr	glass + gar_{ss}	large amounts of gar_{ss}
	glass	1280	3 days	glass + gar_{ss} + pwo	
	xtl	1280	3 days	glass + gar_{ss} + pwo	traces of pwo
	xtl	1270	3 days	glass + gar_{ss} + pwo	
	glass	1265	7 days	gar_{ss}	traces of pwo
	xtl	1250	3 days	gar_{ss}	
$andr_{75}Ti\text{-}gar_{25}$	glass	1300	2 hr	glass	
	glass	1295	2 hr	glass + gar_{ss}	
	glass	1285	3 days	glass + gar_{ss}	
	glass	1280	3 days	glass + gar_{ss} + pwo	
	xtl	1280	3 days	glass + gar_{ss} + pwo	traces of pwo
	xtl	1270	7 days	gar_{ss}	traces of pwo
	glass	1260	5 days	gar_{ss}	
	xtl	1260	7 days	gar_{ss}	traces of pwo
	xtl	1225	8 days	gar_{ss}	
$andr_{72.5}Ti\text{-}gar_{27.5}$	glass	1309	2 hr	glass	
	glass	1305	2 hr	glass + gar_{ss}	small amounts of gar_{ss}
$andr_{70}Ti\text{-}gar_{30}$	glass	1330	2 hr	glass	
	glass	1320	2 hr	glass + pv_{ss}	traces of pv_{ss}
	glass	1315	20 hr	glass + pv_{ss}	traces of pv_{ss}
	xtl	1313	7 days	glass + gar_{ss}	small amount of gar_{ss}
	glass	1310	2 hr	glass + pv_{ss} + gar_{ss}	pv_{ss} corroded
	glass	1300	2 hr	glass + gar_{ss}	traces of pv_{ss}

TABLE 2 (continued)

Composition	Starting material	T, °C	Time	Products	Remarks
$andr_{70}Ti\text{-}gar_{30}$	xtl	1300	4 days	glass + gar_{ss}	
	glass	1285	3 days	glass + gar_{ss}	
	glass	1280	12 days	glass + gar_{ss} + pwo	
	xtl	1280	12 days	glass + gar_{ss} + pwo	
	glass	1275	24 hr	gar_{ss}	traces of pwo
	xtl	1275	24 hr	gar_{ss}	traces of pwo
	glass	1275	3 days	gar_{ss}	
	xtl	1225	7 days	gar_{ss}	
$andr_{67.1}Ti\text{-}gar_{32.9}$	xtl	1365	2 hr	glass	
	xtl	1360	2 hr	glass + pv_{ss}	small amounts of pv_{ss}
	xtl	1320	20 hr	glass + pv_{ss}	
	xtl	1315	20 hr	glass + gar_{ss}	traces of corroded pv_{ss}
	xtl	1310	20 hr	glass + gar_{ss}	
$andr_{64.2}Ti\text{-}gar_{35.8}$	glass	1375	2 hr	glass	
	glass	1370	2 hr	glass + pv_{ss}	small amounts of pv_{ss}
	glass	1320	20 hr	glass + pv_{ss}	
	glass	1315	20 hr	glass + pv_{ss} + gar_{ss}	gar_{ss} in traces and corroded pv_{ss}
	glass	1313	7 days	glass + gar_{ss}	
	glass	1285	3 days	glass + gar_{ss}	
	glass	1280	3 days	gar_{ss}	traces of pwo
	glass	1275	24 hr	gar_{ss}	
	xtl	1275	3 days	gar_{ss}	
$andr_{57}Ti\text{-}gar_{43}$	glass	1400	1 hr	glass	pv_{ss} on quenching
	glass	1350	2 hr	glass + pv_{ss}	
	glass	1320	20 hr	glass + pv_{ss}	
	glass	1315	24 hr	glass + pv_{ss} + gar_{ss}	gar_{ss} in traces and corroded pv_{ss}
	glass	1310	2 days	glass + gar_{ss}	
	glass	1295	4 days	glass + gar_{ss}	glass in small amounts
	xtl	1290	9 days	gar_{ss}	
	glass	1290	9 days	gar_{ss}	
$andr_{53.5}Ti\text{-}gar_{46.5}$	glass	1350	4 days	glass + pv_{ss}	
	glass	1317	3 days	glass + pv_{ss}	
	glass	1315	3 days	glass + pv_{ss} + gar_{ss}	gar_{ss} in traces and corroded pv_{ss}
	xtl	1310	6 days	glass + gar_{ss}	
	glass	1305	6 days	gar_{ss}	
	xtl	1300	6 days	gar_{ss}	
$andr_{50}Ti\text{-}gar_{50}$	glass	1370	2 hr	glass + pv_{ss}	
	glass	1320	20 hr	glass + pv_{ss}	
	glass	1317	3 days	glass + pv_{ss}	
	glass	1315	3 days	glass + pv_{ss} + gar_{ss}	
	glass	1310	3 days	glass + pv_{ss} + gar_{ss}	
	glass	1305	3 days	gar_{ss}	
	xtl	1300	7 days	gar_{ss}	
$andr_{45}Ti\text{-}gar_{55}$	glass	1350	4 days	glass + pv_{ss}	
	glass	1315	6 days	glass + pv_{ss}	
	glass	1310	6 days	glass + pv_{ss} + gar_{ss} + hem	small amounts of hem and glass
	xtl	1305	6 days	pv_{ss} + gar_{ss} + hem	
$andr_{40}Ti\text{-}gar_{60}$	xtl	1350	1 day	glass + pv_{ss} + hem	
	glass	1315	1 day	glass + pv_{ss} + hem	
	glass	1310	2 days	glass + pv_{ss} + hem + gar_{ss}	
	glass	1305	2 days	pv_{ss} + hem + gar_{ss}	
$andr_{31}Ti\text{-}gar_{69}$	glass	1350	1 day	glass + pv_{ss} + hem	
	glass	1315	3 days	glass + pv_{ss} + hem	
	xtl	1310	6 days	pv_{ss} + hem + gar_{ss}	
	glass	1305	1 day	pv_{ss} + hem + gar_{ss}	
$andr_{20}Ti\text{-}gar_{80}$	xtl	1350	3 days	glass + pv_{ss} + hem	
	xtl	1315	7 days	glass + pv_{ss} + hem	

TABLE 2 (continued)

Composition	Starting material	T, °C	Time	Products	Remarks
$andr_{20}Ti\text{-}gar_{80}$	xtl	1310	4 days	pv_{ss} + hem + gar_{ss}	traces of glass
	xtl	1300	3 days	pv_{ss} + hem + gar_{ss}	
$andr_{10}Ti\text{-}gar_{90}$	xtl	1350	4 days	glass + pv_{ss} + hem	
	xtl	1315	7 days	glass + pv_{ss} + hem	traces of glass
	xtl	1310	4 days	pv_{ss} + hem + gar_{ss}	traces of gar_{ss}
	xtl	1225	6 days	pv_{ss} + hem + gar_{ss}	
$andr_{0}Ti\text{-}gar_{100}$	xtl	1350	5 days	pv_{ss} + hem	
	xtl	1310	4 days	pv_{ss} + hem	
	xtl	1250	4 days	pv_{ss} + hem	
	xtl	1200	4 days	pv_{ss} + hem	

Abbreviations: andr, andradite; gar_{ss}, garnet solid solution; hem, hematite; pv_{ss}, perovskite solid solution; pwo, pseudowollastonite; Ti-gar, Ti-garnet; wo, wollastonite; xtl, crystallized material.

TABLE 3

Quenching results for compositions on the join wollastonite-perovskite-hematite

Composition	Starting material	T, °C	Time	Products	Remarks
$wo_{73}pv_{0}hem_{27}$	glass	1320	2 days	glass + pwo	
	glass	1315	2 days	glass + pwo	
	glass	1280	3 days	pwo + hem	
	glass	1250	3 days	pwo + hem	
	xtl	1225	7 days	pwo + hem	
	xtl	1175	7 days	pwo + hem	
	xtl	1100	7 days	wo + gar_{ss}	
$wo_{39}pv_{43}hem_{18}$	glass	1320	3 days	glass + pv_{ss}	
	glass	1315	3 days	glass + pv_{ss}	
	glass	1310	4 days	glass + pv_{ss} + gar_{ss}	
	glass	1300	3 days	glass + pv_{ss} + gar_{ss}	
	xtl	1280	4 days	pv_{ss} + gar_{ss} + pwo	
	xtl	1225	14 days	pv_{ss} + gar_{ss} + pwo	
	xtl	1100	21 days	pv_{ss} + gar_{ss} + wo	
$wo_{48}pv_{27}hem_{25}$	glass	1320	3 days	glass + pv_{ss}	
	glass	1315	2 days	glass + gar_{ss}	traces of gar_{ss}
	glass	1300	3 days	glass + gar_{ss}	
	xtl	1290	4 days	glass + gar_{ss}	
	glass	1290	4 days	glass + gar_{ss}	
	xtl	1280	6 days	gar_{ss} + pwo + pv_{ss}	traces of pv_{ss}
	xtl	1225	14 days	gar_{ss} + pwo + pv_{ss}	traces of pv_{ss}
	xtl	1100	21 days	gar_{ss} + wo	
$wo_{50}pv_{17}hem_{33}$	glass	1300	24 hours	glass	
	glass	1280	3 days	glass + gar_{ss}	small amounts of glass
	xtl	1225	14 days	gar_{ss} + hem	
	xtl	1100	21 days	gar_{ss} + hem	

Abbreviations as in table 2.

Above 1137°C pure andradite is no longer stable as a single phase (Huckenholz, Schairer, and Yoder, 1967), and $garnet_{ss}$ of compositions ranging from $andr_{100}Ti\text{-}gar_{0}$ to $andr_{80}Ti\text{-}gar_{20}$ yield the assemblages pwo + gar_{ss} + hem and pwo + hem before they begin to melt at 1268° ± 2°C. Ti-$garnet_{ss}$ melts incongruently to $perovskite_{ss}$ + liquid at 1315° ± 2°C and at a composition greater than 46.5 percent but less than 50 percent

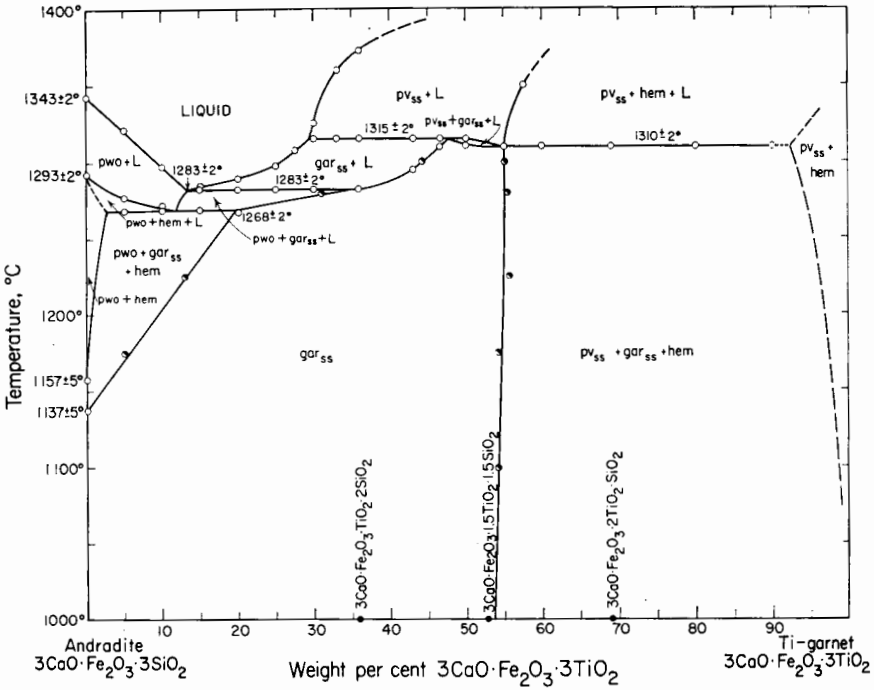

Fig. 3. Temperature versus composition plot of data obtained on the join andradite–Ti-garnet at 1 atm pressure. Abbreviations for phases encountered: gar_{ss}, garnet solid solution; pwo, pseudowollastonite; hem, hematite; and pv_{ss}, perovskite solid solution. Open circles represent data obtained by optical and X-ray determinations; half shaded circles represent data obtained by the determination of the unit-cell parameters of $garnet_{ss}$ (illus. in fig. 4).

by weight of $3CaO \cdot Fe_2O_3 \cdot 3TiO_2$. The composition with the maximum thermal stability is believed to be close to 48 percent, as depicted in figure 2. It was not possible to synthesize an $andradite_{ss}$ containing 69 percent of the Ti-garnet component, believed by Ito and Frondel (1967) to have been synthesized by them. The Ti-garnet component in the $garnet_{ss}$ does not exceed 55 percent by weight, and at compositions greater than 55 percent the polyphase assemblages of $pv_{ss} + gar_{ss} + hem$ or $pv_{ss} + hem$ are formed. The latter assemblage is restricted to a composition less than $andr_{7}Ti\text{-}gar_{93}$.

In order to set up suitable determinative procedures for $Ti\text{-}andradite_{ss}$ the unit-cell parameter a_0 was measured on garnets along the join andradite–Ti-garnet with the use of material that had been held at temperatures of 1100°, 1175°, 1225°, 1280°, and 1300°C for periods of time required to obtain equilibrium (fig. 4 and table 4). The high-angle reflections (640) and (642) of the $garnet_{ss}$ were measured against the (300) and (024) reflections of $KBrO_3$, which are located at 52.723° and 57.391° 2θ Cukα respectively, for the entire range of the $Ti\text{-}andradite_{ss}$ obtained in this study. Two patterns were run for a single garnet com-

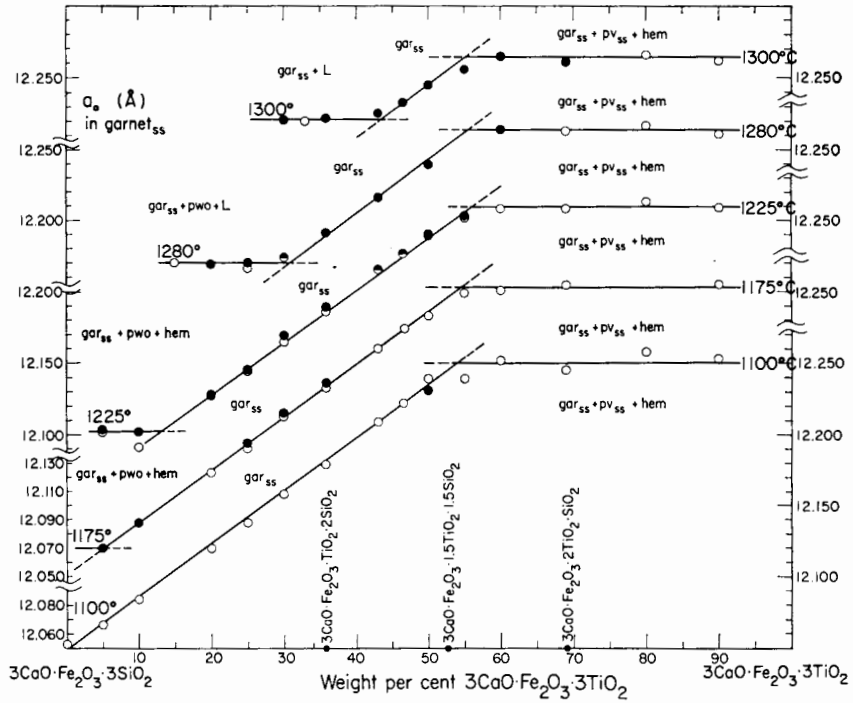

Fig. 4. Unit-cell parameters of garnets from compositions along the join andradite–Ti-garnet treated at temperatures as indicated in the diagram. Starting materials used are garnets crystallized at 1050°C (open circles) or fine-powdered glasses (solid circles). Abbreviations as in figure 3.

position, and the diffraction chart was read ten times for every peak. The readings are reproducible to better than 0.01°2θ, and the difference between a_o calculated from (642) and (640) is rarely larger than 0.003Å.

The cell parameter for pure andradite synthesized at 1 atm was recently determined by Huckenholz and others (1967) as 12.053 ± 0.003 Å, with the use of the reflections (642), (640), (611), (521), (510), (422), (420), and (400), with silicon as an internal standard. The increase of the cell parameter from andr$_{100}$ Ti-gar$_0$ to andr$_{45}$ Ti-gar$_{55}$ is 0.038 ± 0.002 Å per 10 wt percent and 0.040 ± 0.002 Å per mole percent. The cell dimensions reported by Ito and Frondel (1967) for five Ti-andradites synthesized along the join andradite–Ti-garnet at 1050°C lie close to the 1100°C unit-cell curve of this study (fig. 4). Their cell dimensions indicate, on the basis of the present interpretation, a termination of the garnet solid solution between 56 and 59 wt percent (=84 to 88 mole percent of Ito and Frondel's scale). The determination of the cell parameters is a very helpful means of obtaining garnet compositions in polyphase assemblages, and the cell parameter a_o has been used in mapping field boundaries on the binary join andradite–Ti-garnet as well as in the

TABLE 4

Unit-cell parameters of garnets from compositions along the join andradite—Ti-garnet

Composition	Starting material	a_o (in Å) of garnet$_{ss}$ crystallized at temperatures of 1100°C	1175°C	1225°C	1280°C	1300°C
$andr_{100}Ti\text{-}gar_0$	xtl	12.053	...	...	...	...
	glass	...	...	...	...	...
$andr_{95}Ti\text{-}gar_5$	xtl	12.066	...	12.101*	...	...
	glass	...	12,070	12.103*	...	...
$andr_{90}Ti\text{-}gar_{10}$	xtl	12.084	...	12.092*	...	...
	glass	...	12.088	12.102*	...	...
$andr_{85}Ti\text{-}gar_{15}$	xtl	...	...	...	12.170**	...
	glass	...	...	...	...	...
$andr_{80}Ti\text{-}gar_{20}$	xtl	12.120	12.123	12.127	12.169**	...
	glass	...	...	12.128	...	...
$andr_{75}Ti\text{-}gar_{25}$	xtl	12.138	12.140	12.146	12.167**	...
	glass	...	12.144	12.145	12.170**	...
$andr_{70}Ti\text{-}gar_{30}$	xtl	12.158	12.163	12.165	12.174**	...
	glass	...	12.165	12.169	12.174**	12.221***
$andr_{67.1}Ti\text{-}gar_{32.9}$	xtl	...	...	...	...	12.220***
	glass	...	...	...	...	...
$andr_{64.2}Ti\text{-}gar_{35.8}$	xtl	12.179	12.183	12.186	...	...
	glass	...	12.186	12.189	12.191	12.222***
$andr_{57}Ti\text{-}gar_{43}$	xtl	12.209	12.210	12.217	...	...
	glass	...	...	12.217	12.216	12.226***
$andr_{53.5}Ti\text{-}gar_{46.5}$	xtl	12.222	12.224	12.227	...	...
	glass	...	...	12.227	...	12.233
$andr_{50}Ti\text{-}gar_{50}$	xtl	12.239	12.233	12.239	...	...
	glass	12.231	...	12.240	12.238	12.245
$andr_{45}Ti\text{-}gar_{55}$	xtl	12.239†	12.249†	12.252	...	...
	glass	...	...	12.253	...	12.256
$andr_{40}Ti\text{-}gar_{60}$	xtl	12.252†	12.251†	12.258†	...	...
	glass	...	...	...	12.264†	12.265†
$andr_{31}Ti\text{-}gar_{69}$	xtl	12.245†	12.255†	12.258†	12.263†	...
	glass	...	...	...	...	12.261†
$andr_{20}Ti\text{-}gar_{80}$	xtl	12.258†	...	12.263†	12.267†	12.266†
	glass	...	...	...	...	...
$andr_{10}Ti\text{-}gar_{90}$	xtl	12.253†	12.255†	12.259†	12.261†	12.262†
	glass	...	...	...	...	...

*assemblage: gar_{ss} + pwo + hem.

**assemblage: gar_{ss} + pwo + L.

***assemblage: gar_{ss} + L.

†assemblage: gar_{ss} + pv_{ss} + hem.

Abbreviations as in table 2.

ternary system wo-pv-hem (table 5). However, at compositions more Ti-rich than $andr_{45}Ti\text{-}gar_{55}$ and in the assemblage $pv_{ss} + gar_{ss} +$ hem in which hematite is present in larger amounts, the (640) reflection of the garnet cannot be read with great precision. The hematite reflection $(11\bar{2}6)$ at 53.88°2θ coincides with that of the $garnet_{ss}$ (640). In these determinations the (642) reflection of the garnet has been measured four times.

TABLE 5

Unit-cell parameters of garnets from compositions on the join wollastonite-perovskite-hematite

Composition	Starting material	a_o (in Å) of $garnet_{ss}$ crystallized at temperatures of 1100°C	1175°C	1225°C	1280°C	1300°C
$wo_{39}pv_{43}hem_{18}$	xtl	12.205	...	12.210	...	...
	glass	...	...	...	12.212	12.223
$wo_{48}pv_{27}hem_{25}$	xtl	12.179	...	12.185	...	12.218
	glass	...	...	...	...	...
$wo_{50}pv_{17}hem_{33}$	xtl	12.133	...	12.137	...	...
	glass	...	...	...	12.159	...

The liquidus phases on the join andradite–Ti–garnet are pseudowollastonite, $garnet_{ss}$, and $perovskite_{ss}$. The composition of the garnet that appears on the liquidus is restricted between $andr_{86}Ti\text{-}gar_{14}$ and $andr_{71}Ti\text{-}gar_{29}$. $Garnet_{ss}$ reacts at temperatures higher than 1315° ± 2°C to $pv_{ss} +$ liquid when the time is sufficient (>2 hours) to obtain equilibrium. Primary perovskite contains small amounts of silicon and traces of iron, as determined qualitatively by microprobe analyses, indicating a limited solid solution of $CaO \cdot SiO_2$ in the perovskite. Above 1315°C the amount of $perovskite_{ss}$ in the glass is small; below that temperature $garnet_{ss}$ is very abundant, and the amount of glass becomes considerably smaller approaching the solidus of the $garnet_{ss}$. A quaternary univariant line pierces the join andradite–Ti-garnet at 1310° ± 2°C and 55 wt percent. The piercing point may be considered as a ternary invariant point because $perovskite_{ss}$, $garnet_{ss}$, hematite, and liquid are in equilibrium, assuming that all compositions lie on the join wo-hem-pv or very close to it.

However, the join andradite–Ti-garnet of the wo–hem–pv plane is not strictly binary. Ferrous iron is present, in amounts depending on the temperature and composition (table 6 and fig. 5). The amounts are trifling at 1100° and 1250°C. They are in the order of 1 and 2 percent FeO of the total Fe_2O_3, respectively. Ferrous iron increases with temperature, and mixtures quenched from 1500°C contain about 14 percent iron in the ferrous state. Nevertheless, the amounts of ferrous iron in the runs are considered to be small under the temperature conditions applied in the quenching experiments, and the join is treated as binary in this study.

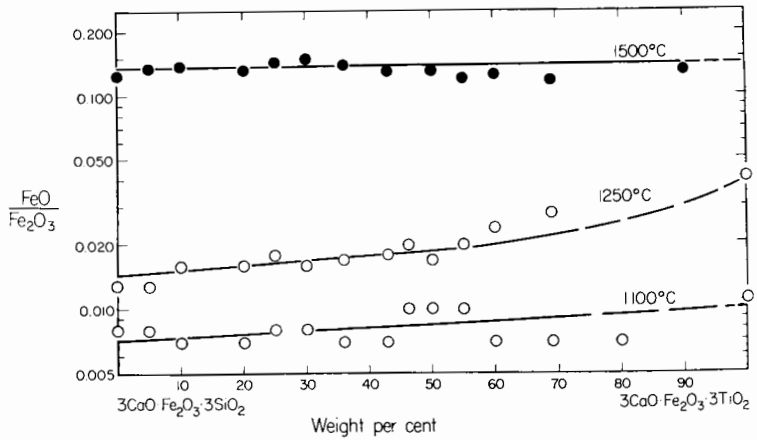

Fig. 5. FeO/Fe_2O_3 versus composition plot of data along the join andradite–Ti-garnet. Open circles represent data obtained for crystalline material which was held at temperatures of 1100° and 1250°C for several weeks; solid circles represent data for starting mixtures which were quenched from 1500°C.

TABLE 6

Amounts of FeO present in compositions along the join andradite—Ti-garnet and in the plane wo-hem-pv at various temperatures

Composition	Percentage total iron as Fe_2O_3	Percentage FeO at 1100°C	1250°C	1500°C	FeO/Fe_2O_3 at 1100°C	1250°C	1500°C
$andr_{100}Ti\text{-}gar_0$	31.44	0.25	0.40	3.95	0.008	0.013	0.125
$andr_{95}Ti\text{-}gar_5$	31.27	0.25	0.40	4.20	0.008	0.013	0.135
$andr_{90}Ti\text{-}gar_{10}$	31.11	0.20	0.50	4.30	0.007	0.016	0.138
$andr_{80}Ti\text{-}gar_{20}$	30.78	0.20	0.50	4.10	0.007	0.016	0.133
$andr_{75}Ti\text{-}gar_{25}$	30.61	0.25	0.55	4.40	0.008	0.018	0.144
$andr_{70}Ti\text{-}gar_{30}$	30.45	0.25	0.50	4.60	0.008	0.016	0.151
$andr_{64.2}Ti\text{-}gar_{35.8}$	30.25	0.20	0.50	4.20	0.007	0.017	0.139
$andr_{57}Ti\text{-}gar_{43}$	30.02	0.20	0.55	3.90	0.007	0.018	0.130
$andr_{53.5}Ti\text{-}gar_{46.5}$	29.90	0.30	0.60	n.b.	0.010	0.020	...
$andr_{50}Ti\text{-}gar_{50}$	29.78	0.30	0.50	3.90	0.010	0.017	0.131
$andr_{45}Ti\text{-}gar_{55}$	29.63	0.30	0.60	3.50	0.010	0.020	0.118
$andr_{40}Ti\text{-}gar_{60}$	29.45	0.20	0.70	3.65	0.007	0.024	0.124
$andr_{31}Ti\text{-}gar_{69}$	29.15	0.20	n.b.	3.40	0.007	...	0.117
$andr_{20}Ti\text{-}gar_{80}$	28.79	0.20	0.80	n.b.	0.007	0.028	...
$andr_{10}Ti\text{-}gar_{90}$	28.46	n.b.	n.b.	3.60	...	...	0.127
$andr_0Ti\text{-}gar_{100}$	28.13	0.30	1.15	n.b.	0.011	0.041	...
wo48hem25pv27	25.00	0.20	0.55	3.60	0.008	0.022	0.144
wo39hem18pv43	18.00	0.15	0.20	1.15	0.008	0.011	0.064
wo50hem33pv17	33.00	0.25	n.b.	3.30	0.008	...	0.100

Abbreviations as in table 2.

ISOTHERMAL SECTIONS

In order to elucidate the phase relationships in the ternary system wollastonite ($CaO \cdot SiO_2$)–perovskite ($CaO \cdot TiO_2$)–hematite (Fe_2O_3), a series of isothermal sections at 1320°, 1312°, 1300°, 1280°, 1225°, 1175°, and 1100°C are presented. At 1320°C (fig. 6) the stable phase assemblages on the join wo–pv–hem are L, hem + L, hem + pv_{ss} + L, hem + pv_{ss}, pv_{ss} + L, pwo + pv_{ss} + L, and pwo + L. $Garnet_{ss}$ appears on the join

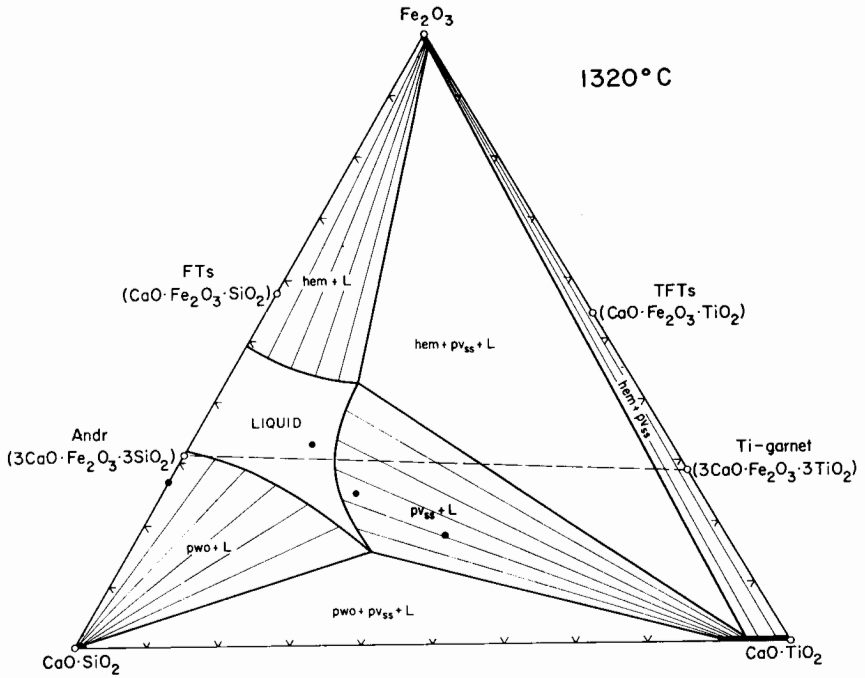

Fig. 6. Isothermal section of the wollastonite ($CaO \cdot SiO_2$)–perovskite ($CaO \cdot TiO_2$)–hematite (Fe_2O_3) join at 1320°C. Here and in the following isothermal sections phase relationships along the join $CaO \cdot SiO_2$–$CaO \cdot TiO_2$ are not shown.

by the reaction perovskite$_{ss}$ + liquid → garnet$_{ss}$ at 1315° ± 2°C. Figure 7 depicts a condition slightly below this temperature. As can be seen, perovskite$_{ss}$ is in equilibrium with a liquid either rich or poor in Fe_2O_3. At 1300°C (fig. 8) phase assemblages of gar$_{ss}$ with either hem or pv$_{ss}$, or both, occur, because perovskite$_{ss}$ is no longer in coexistence with the liquid rich in Fe_2O_3. The temperature for this reaction is 1310° ± 2°C, and at this temperature the liquid, garnet$_{ss}$, and perovskite$_{ss}$ lie on or very close to a straight line. The three solid phases gar$_{ss}$, pv$_{ss}$, and hem, as well as the liquid, are in equilibrium, and a ternary invariant point appears in figure 3. The assemblages pv$_{ss}$ + *L* (Fe_2O_3-poor) and pv$_{ss}$ + gar$_{ss}$ + *L* (Fe_2O_3-poor), still present at 1300° (and 1290°C), have disappeared before the liquid reaches the binary join andradite–Ti-garnet at 1283° ± 2°C. Pwo + gar$_{ss}$ + pv$_{ss}$ and pwo + gar$_{ss}$ become the stable phase assemblages, and the liquid region lies wholly on the Fe_2O_3-rich side of the binary join andradite–Ti-garnet (fig. 9). The liquid disappears from the ternary join wollastonite–perovskite–hematite between 1280° and 1225°C. The temperature was fixed in figure 3 at 1268° ± 2°C. From 1225°C (fig. 10) there is a substantial increase of the garnet$_{ss}$ series, which almost reaches the join wo-hem in the 1175°C section (fig. 11). The garnet$_{ss}$ has closed the gap at 1100°C (fig. 12). The temperature

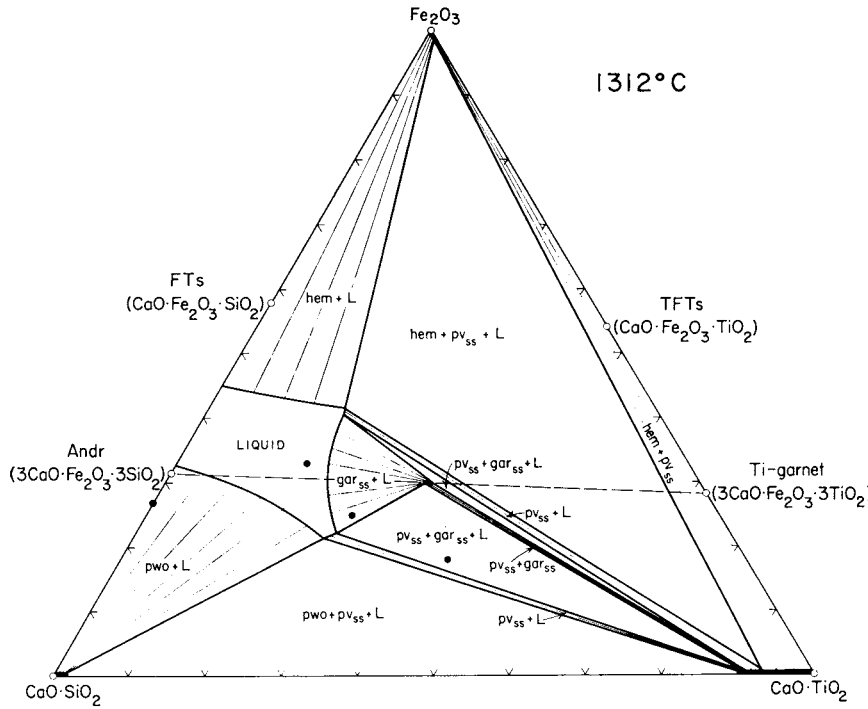

Fig. 7. Isothermal section of the wollastonite ($CaO \cdot SiO_2$)–perovskite ($CaO \cdot TiO_2$)–hematite (Fe_2O_3) join at 1312°C.

for this closure is the upper stability of pure andradite (Huckenholz, and others, 1967).

THE JOIN DIOPSIDE—TITANIUM FERRI-TSCHERMAK'S MOLECULE

In addition to the ternary join wollastonite-perovskite-hematite, a series of compositions were studied along the binary join diopside ($CaO \cdot MgO \cdot 2SiO_2$)–titanium ferri-Tschermak's molecule ($CaO \cdot TiO_2 \cdot Fe_2O_3$) on the plane diopside–perovskite–hematite, within the enstatite-wollastonite-perovskite-hematite system (fig. 1), in order to obtain information about the phase relationships of clinopyroxene and garnet. The stable phases along the join diopside (di)–titanium ferri-Tschermak's molecule (TFTs) are clinopyroxene solid solution (cpx_{ss}), garnet solid solution (gar_{ss}), hematite (hem), and perovskite solid solution (pv_{ss}) (table 7 and fig. 13). From the results obtained clinopyroxene$_{ss}$ and magnetite$_{ss}$ appear on the liquidus in the di-rich part of the join. Clinopyroxene$_{ss}$ forms stout prisms of about 10 to 20 microns in length, shows fine lamella-twinning and anomalous extinction. Its color is slightly yellow. Magnetite occurs as small euhedral crystals. Clinopyroxene$_{ss}$, garnet$_{ss}$, hematite, and perovskite$_{ss}$ form fine-grained intergrowths in the polyphase assemblages, which rarely exceed grain sizes of more than 5 microns.

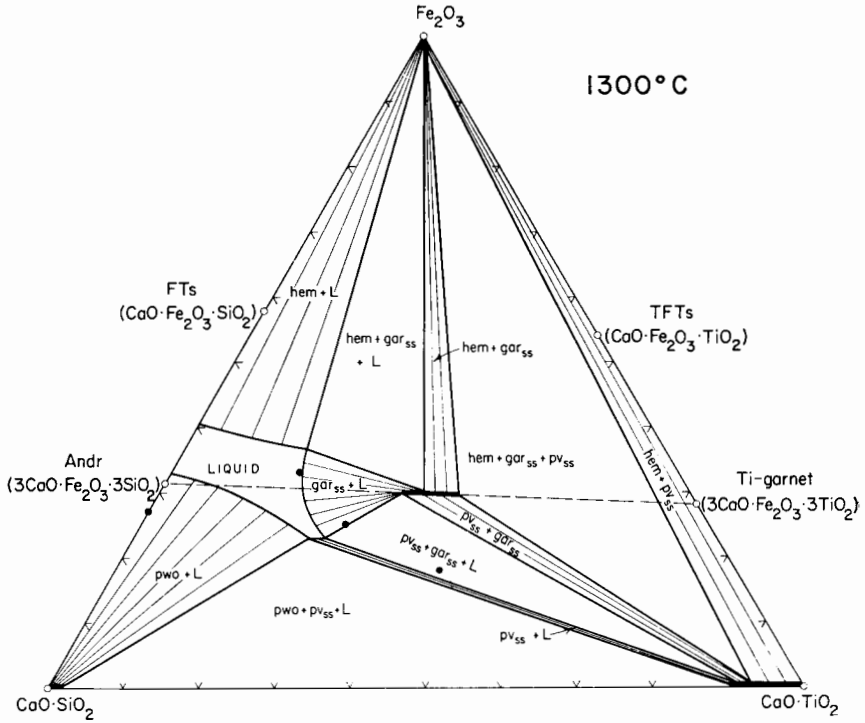

Fig. 8. Isothermal section of the wollastonite ($CaO \cdot SiO_2$)–perovskite ($CaO \cdot TiO_2$)–hematite (Fe_2O_3) join at 1300°C.

There is a very limited range of solid solution of TFTs in the diopside. The solid solution is less than 5 wt percent TFTs and is believed to be of the order of 2 percent at temperatures between 1000° and 1150°C. Beyond 2 percent TFTs, clinopyroxene$_{ss}$ is no longer stable as a single phase, and assemblages of cpx_{ss} + gar_{ss}, cpx_{ss} + gar_{ss} + hem, cpx_{ss} + gar_{ss} + hem + pv_{ss}, gar_{ss} + hem + pv_{ss}, and hem + pv_{ss} are intersected by the join di–TFTs.

The cpx_{ss} in the polyphase assemblages cannot lie on the plane di-pv-hem, because tie lines from garnet solid solutions on or close to the plane wo-pv-hem in the en-wo-pv-hem system to diopside do not intersect the plane di-pv-hem. For this reason the cpx_{ss} composition must contain the enstatite component. A least-squares refinement of X-ray diffraction measurements was carried out on the clinopyroxene$_{ss}$ of the composition $di_{80}TFTs_{20}$, which was treated at 1150°C for 8 days. The cell parameters ($a = 9.78 \pm 0.02$ Å, $b = 8.94 \pm 0.01$ Å, $c = 5.29 \pm 0.02$ Å, $V = 443.7 \pm 1.4$ Å^3) agree with these obtained for ferri-diopside$_{ss}$ (Huckenholz, Schairer, and Yoder, 1967) within the limits of error. However, the angle β (106.08 ± 0.16°) indicates that the clinopyroxene is not simply ferri-diopside but a member of the diopside-enstatite solid solution series (Clark, Schairer, and de Neufville, 1962) as well. The substitution of Mg for Ca in eight-fold positions is indicated by an increase of β com-

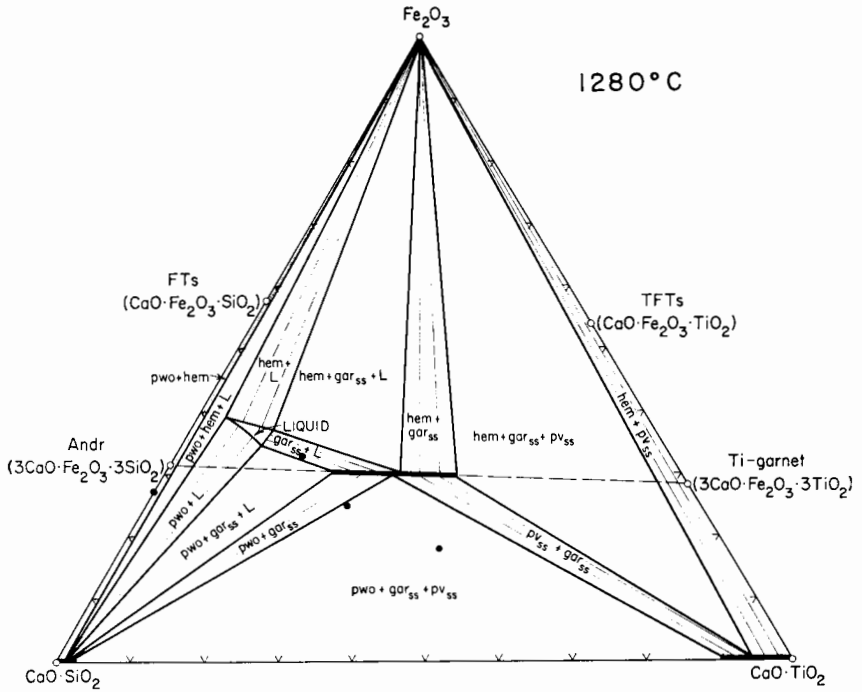

Fig. 9. Isothermal section of the wollastonite ($CaO \cdot SiO_2$)–perovskite ($CaO \cdot TiO_2$)–hematite (Fe_2O_3) join at 1280°C.

pared with pure diopside and ferri-diopside. Therefore, the clinopyroxene$_{ss}$ in coexistence with garnet$_{ss}$ is considered to be of diopside composition, containing both ferri-Tschermak's and enstatite molecules in solid solution.

The cell edges of the garnet along the join di–TFTs are 12.170 and 12.180 Å in the two-phase volume cpx$_{ss}$ + gar$_{ss}$, and 12.207, 12.208, and 12.201 Å in the three-phase volume cpx$_{ss}$ + gar$_{ss}$ + hem, respectively. These cell edges refer to the solid solution series of andradite–Ti-garnet. However, the relationship will probably change if Mg enters the andradite structure. There is a very limited substitution for andradite ($3CaO \cdot Fe_2O_3 \cdot 3SiO_2$) of khoharite ($3MgO \cdot Fe_2O_3 \cdot 3SiO_2$) as demonstrated by Huckenholz, Schairer, and Yoder, 1967. The substitution of $MgTi^{4+}$ for $2Fe^{3+}$ was tested for this investigation along the join andradite ($3CaO \cdot Fe_2O_3 \cdot 3SiO_2$)–Mg-melanite ($3CaO \cdot MgO \cdot TiO_2 \cdot 3SiO_2$) (fig. 1). Compositions of andr$_{66.7}$Mg-mela$_{33.3}$ and andr$_0$ Mg-mela$_{100}$ were treated at temperatures of 1050°, 1150°, and 1200°C (table 8). Polyphase assemblages of garnet$_{ss}$ + wollastonite + melilite$_{ss}$ and of clinopyroxene$_{ss}$ + perovskite$_{ss}$ + melilite$_{ss}$, respectively, were obtained as fine-grained intergrowths under the applied conditions. The garnet of the andr$_{66.7}$Mg-mela$_{33.3}$ composition treated at 1150°C has a cell edge of 12.129 ± 0.003 Å. It cannot be unambiguously ascertained, whether this garnet$_{ss}$ belongs

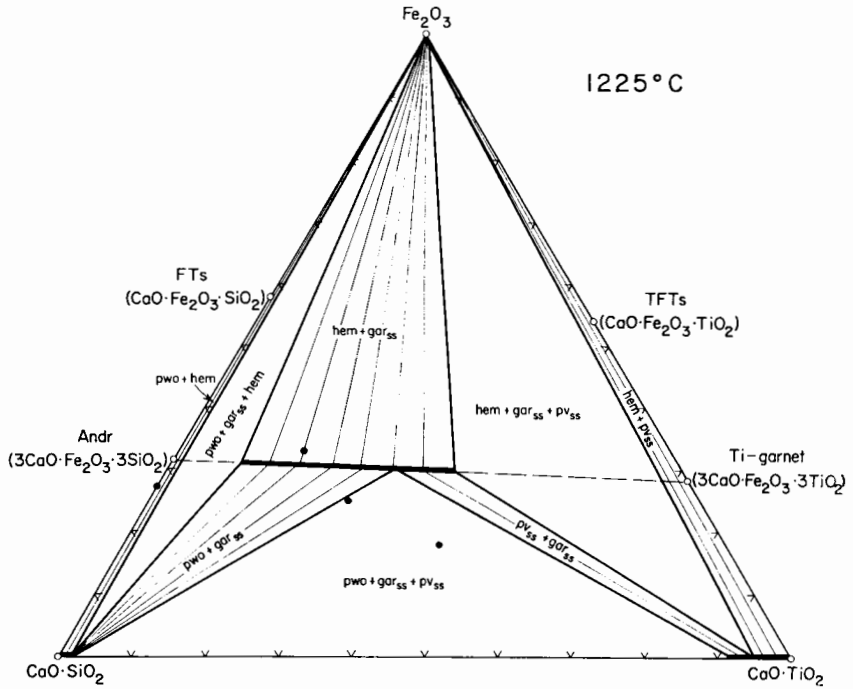

Fig. 10. Isothermal section of the wollastonite ($CaO \cdot SiO_2$)–perovskite ($CaO \cdot TiO_2$)–hematite (Fe_2O_3) join at 1225°C.

to the solid solution series of andradite–Ti-garnet or of andradite–Ti-garnet–Mg-melanite. The substitution of $MgTi^{4+}$ for $2Fe^{3+}$ will not substantially change the cell edge of the $garnet_{ss}$ because the interatomic distances of O to Fe^{3+} (Fe^{3+}–O = 2.01 Å), Mg (Mg–O = 2.07 Å) and Ti^{4+} (Ti^{4+}–O = 2.01 Å) for six-fold coordination are very similar. At present, garnets stable on the joins andradite–Mg-melanite and di–TFTs are considered to be members of an andradite–Ti-garnet–Mg-melanite solid solution series containing less than 33.3 wt percent of a Mg-melanite component. The Mg-melanite component does not appear to exceed 20 wt percent in natural Ti-rich garnets.

GEOLOGIC DISCUSSION

The most common rock types in which Ti-bearing garnets are abundant minerals belong to the nepheline syenite and ijolite families. They are often directly related to carbonatites and their alteration products, the fenites. The main feature of these rocks is the presence of the mafic mineral association of clinopyroxenes and of Ti-bearing garnets (reported as melanite, schorlomite, and iiaavarite). Wollastonite, perovskite, and iron ores (magnetite, titanomagnetite, ilmenite, and occasionally hematite) are sometimes abundant phases too. Biotite, amphibole and sphene may occur in addition.

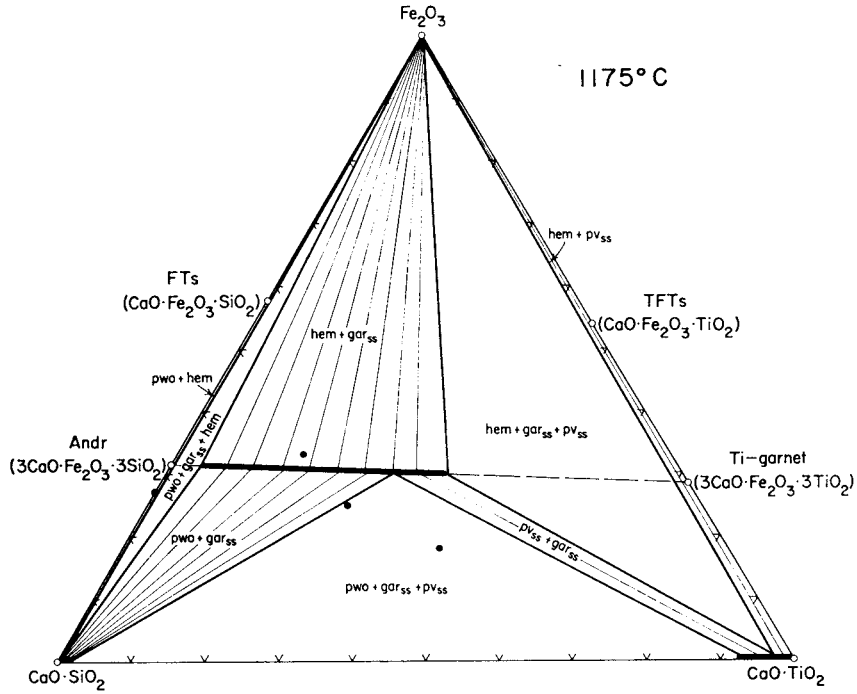

Fig. 11. Isothermal section of the wollastonite ($CaO \cdot SiO_2$)–perovskite ($CaO \cdot TiO_2$)–hematite (Fe_2O_3) join at 1175°C.

The composition of the clinopyroxene varies from aegirine or aegirine-augite to diopside sometimes rich in ferri-Tschermak's molecule. Even pigeonitic augites are reported from a pyroxenite and foyaite-porphyrite dike which contains melanite, from Alnö, Sweden (von Eckermann, 1948, p. 61 and 91). The associated garnet is andraditic in composition is most cases and contains other components in addition, as illustrated in table 1. As it may be seen from the grandite–melanite–Mg,Fe-melanite plot of figure 14, garnets from alkaline plutonic and alkaline hypabyssal rocks contain larger amounts of the Mg,Fe-melanite component compared to their volcanic equivalents. Plutonic and hypabyssal crystallization probably favors the formation of the Mg,Fe-melanite component in Ti-bearing garnets.

The inspection of 61 analyses of Ti-bearing garnets indicates that a relatively high Ti content in addition to Fe^{3+} is always related to a low content of Al. This is in direct contrast to the associated pyroxenes: their Ti-content increases with increasing Al, a behavior outlined in general for clinopyroxenes by Kushiro (1960). Unfortunately, data about coexisting clinopyroxenes and garnets from alkaline igneous rock are rare. Examples are known from ijolites at Iron Hill, Colorado (Larsen, 1942), ijolites from the Napak Volcanoes, Uganda (King, 1949), ijolites

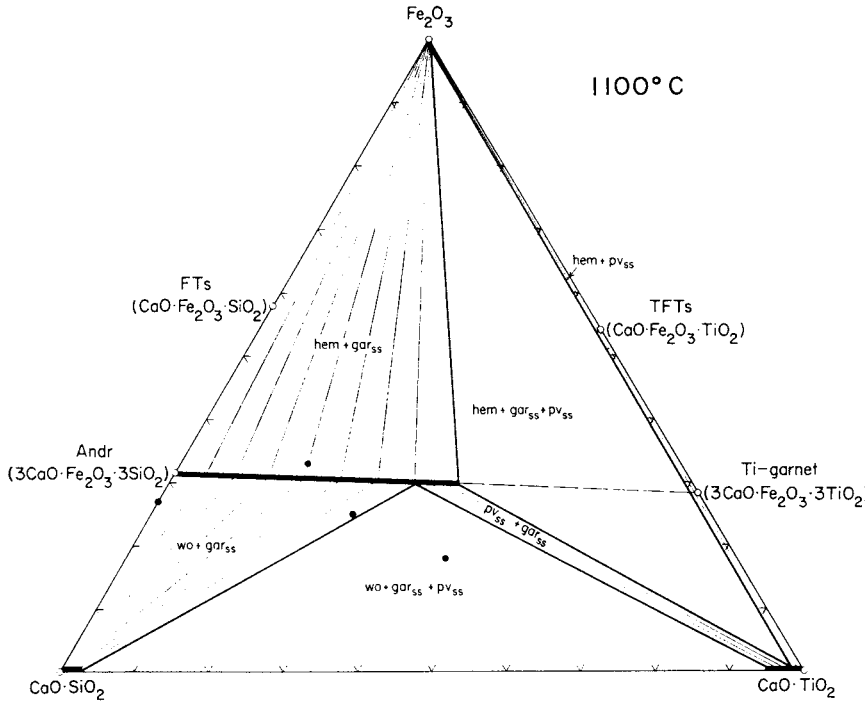

Fig. 12. Isothermal section of the wollastonite ($CaO \cdot SiO_2$)–perovskite ($CaO \cdot TiO_2$)–hematite (Fe_2O_3) join at 1100°C.

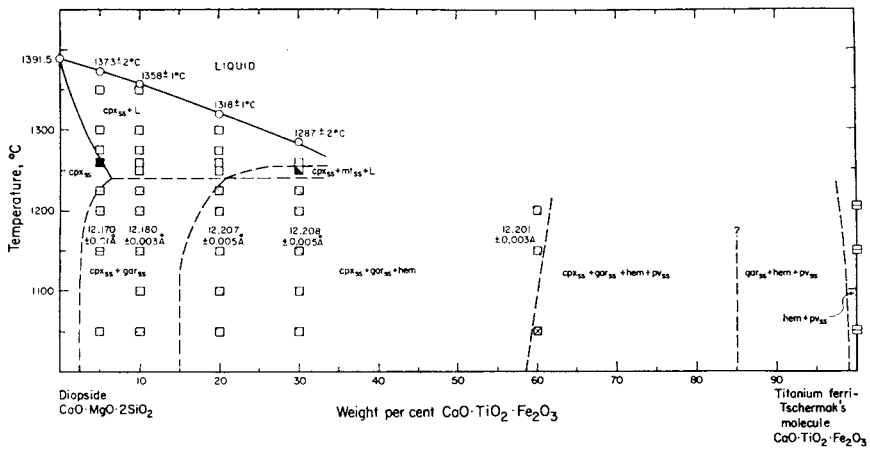

Fig. 13. Temperature versus composition plot of data obtained on the join diopside–titanium ferri-Tschermak's molecule at 1 atm. Abbreviations of phases encountered: cpx_{ss}, clinopyroxene solid solution; gar_{ss} garnet solid solution; hem, hematite; mt_{ss}, magnetite solid solution; and pv_{ss}, perovskite solid solution. Numbers refer to the unit-cell parameters of the coexisting garnet solid solutions.

from the alkalic igneous complex at Magnet Cove, Arkansas (Erickson and Blade 1963), and from a wollastonite-melanite melteigite from the alkaline complex at Oka, Quebec (Gold, 1966). The coexisting minerals or minerals from different hand specimens of similar rocks are plotted on an atomic Ti-Fe^{3+}-Al basis in figure 15. It can be seen that the Napak garnet, relatively high in Al, has a very low content of Ti. The Magnet Cove garnet is low in Al but is very high in Ti. An intermediate position is held by the garnet from Iron Hill. The Oka garnet is almost a pure andradite, having a low Ti-content and only traces of Al. It can be concluded, therefore, that Al-rich grandite is not expected to be rich in Ti.

TABLE 7

Quenching results for compositions along the join diopside—titanium ferri-Tschermak's molecule

Composition	Starting material	T, °C	Time	Products	Remarks
$di_{95}TFTs_5$	glass	1375	2 hr	glass	
	glass	1370	2 hr	glass + cpx_{ss}	twinned cpx_{ss}
	xtl	1275	4 days	glass + cpx_{ss}	twinned cpx_{ss}; traces of glass
	xtl	1260	5 days	cpx_{ss}	
	xtl	1225	7 days	cpx_{ss} + gar_{ss}	traces of gar_{ss}
	xtl	1200	5 days	cpx_{ss} + gar_{ss}	
$di_{90}TFTs_{10}$	xtl	1360	3 hr	glass	
	xtl	1355	3 hr	glass + cpx_{ss}	
	xtl	1250	24 hr	glass + cpx_{ss}	
	xtl	1225	5 days	cpx_{ss} + gar_{ss}	
$di_{80}TFTs_{20}$	xtl	1320	2 hr	glass	
	xtl	1315	2 hr	glass + cpx_{ss}	
	xtl	1250	2 days	glass + cpx_{ss}	
	xtl	1225	5 days	cpx_{ss} + gar_{ss} + hem	small amount of hem
	xtl	1200	5 days	cpx_{ss} + gar_{ss} + hem	
$di_{70}TFTs_{30}$	xtl	1290	2 hr	glass	
	xtl	1285	2 hr	glass + cpx_{ss}	
	xtl	1260	7 days	glass + cpx_{ss}	
	xtl	1250	2 days	glass + cpx_{ss} + mt_{ss}	
	xtl	1225	5 days	gar_{ss} + cpx_{ss} + hem	
$di_{40}TFTs_{60}$	xtl	1200	3 days	cpx_{ss} + gar_{ss} + hem	
	xtl	1150	3 days	cpx_{ss} + gar_{ss} + hem	
	xtl	1050	10 days	cpx_{ss} + gar_{ss} + hem + pv_{ss}	
di_0TFTs_{100}	xtl	1200	3 days	hem + pv_{ss}	
	xtl	1150	3 days	hem + pv_{ss}	
	xtl	1050	10 days	hem + pv_{ss}	

Abbreviations: cpx_{ss}, clinopyroxene solid solution; di, diopside; mt_{ss}, magnetite solid solution; TFTs, titanium ferri-Tschermak's molecule; other abbreviations as in table 2.

The phase relationships in the ternary joins diopside–wollastonite–hematite (Huckenholz, Schairer, and Yoder, 1967), wollastonite–perovskite–hematite, and diopside–perovskite–hematite, and the binary join andradite–Mg-melanite as well as the behavior of natural clinopyroxenes under oxidizing condition (Huckenholz, 1968) bear directly on the formation of andradite and its Ti-rich varieties under magmatic conditions. The results of these studies suggest the concept that the appearance of Ti-bearing garnets and ferri-diopsides is the natural consequence of crys-

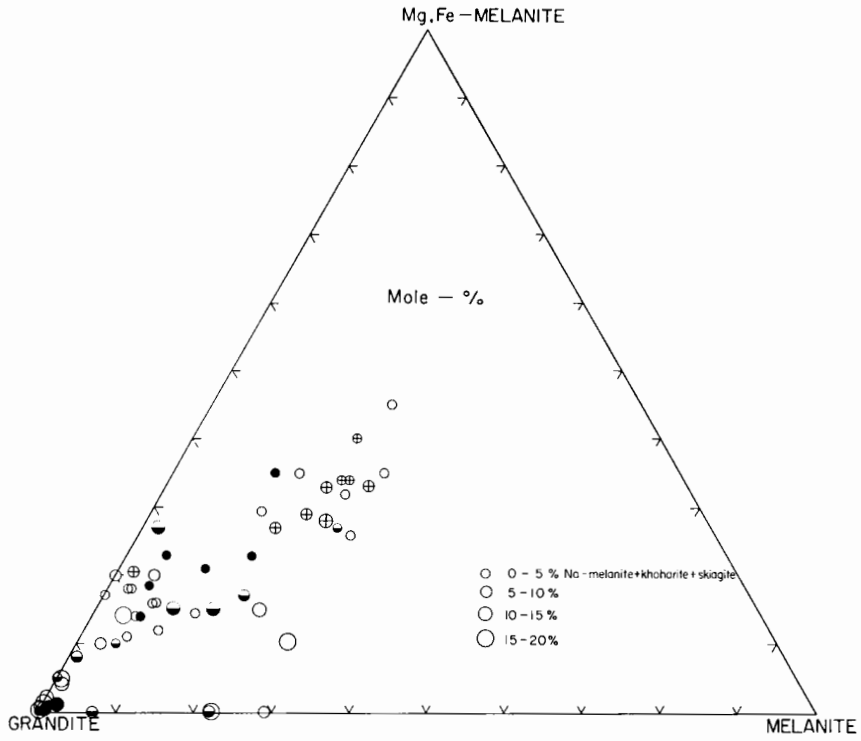

Fig. 14. Grandite ($3CaO \cdot Fe_2O_3 \cdot 3SiO_2 + 3CaO \cdot Al_2O_3 \cdot 3SiO_2$)–melanite ($3CaO \cdot Fe_2O_3 \cdot 3TiO_2$)–Mg, Fe-melanite ($3CaO \cdot MgO \cdot TiO_2 \cdot 3SiO_2 + 3CaO \cdot FeO \cdot TiO_2 \cdot 3SiO_2$) plot of Ti-bearing garnets from metamorphic (solid circles), alkaline plutonic (open circles), alkaline volcanic (half shaded circles), and alkaline hypabyssal rocks (circles with crosses). Analyses were taken from references listed in figure 1 and recalculated with the use of procedure outlined on p. 210.

tallization at or near atmospheric conditions and is not necessarily the result of unique deep-seated processes.

TABLE 8

Preliminary quenching results for compositions along the join andradite—Mg-melanite

Composition	Starting material	T, °C	Time, days	Products
$andr_0Mg\text{-}mela_{100}$	xtl	1200	5	$cpx_{ss} + pv_{ss} + mel_{ss}$
	xtl	1150	6	$cpx_{ss} + pv_{ss} + mel_{ss}$
	xtl	1050	14	$cpx_{ss} + pv_{ss} + mel_{ss}$
$andr_{66.7}Mg\text{-}mela_{33.3}$	xtl	1200	5	$gar_{ss} + wo_{ss} + mel_{ss}$
	xtl	1150	6	$gar_{ss} + wo_{ss} + mel_{ss}$
	xtl	1050	10	$gar_{ss} + wo_{ss} + mel_{ss}$

Abbreviations: mel_{ss}, melilite solid solution; others as in tables 2 and 7.

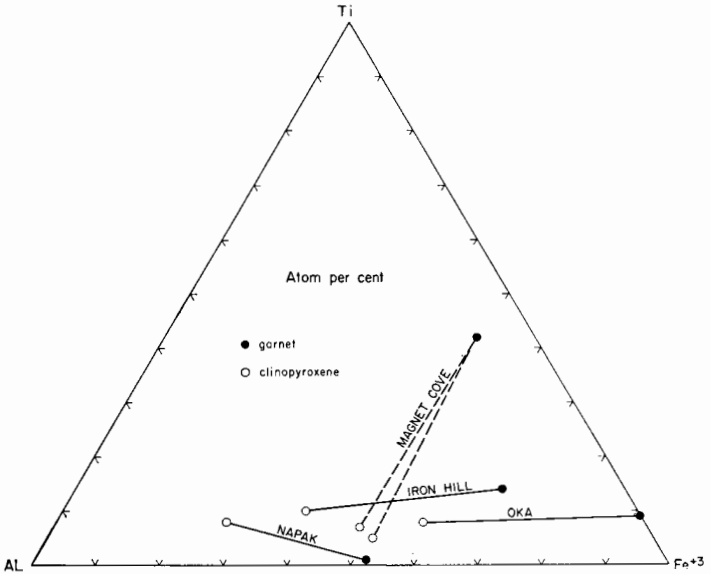

Fig. 15. Coexisting clinopyroxenes and Ti-bearing garnets from alkaline igneous complexes: (1) Iron Hill, Colorado; sodian-augite and melanite from ijolite IH-129 (Larsen, 1942). (2) Napak, Uganda; aegirine-augite and melanite from ijolite K.352 and K.372 respectively (King, 1949). (3) Magnet Cove, Arkansas; diopside from biotite-garnet ijolite L-123-6 and L-123-7, garnet from biotite-garnet ijolite MC-216-8 (Erickson and Blade, 1963). (4) Oka, Quebec; sodian-augite and melanite from wollastonite-melanite melteigite DDH G 14, 330 feet (Gold 1966).

ACKNOWLEDGMENTS

The writer is indebted to Dr. J. F. Schairer and Dr. H. S. Yoder, Jr. for their help and guidance throughout the study and for their kindness in reviewing the manuscript.

REFERENCES

Brauns, R., 1922, Die Mineralien der Niederrheinischen Vulkangebiete: Stuttgart, E. Schweizerbart'sche Verlagsbuchhandlung (Erwin Nägele), 225 p.

Carpanese, T., 1932, Granato, vesuviana, ilmenite e titanite del Monte Rosso di Varra (gruppo del Monte Rosa): Real Acad. Lincei Atti, Cl. Sci. Fis. mat. nat., ser. 6, v. 15, p. 591-595, 694-699.

Clark, S. P., Jr., 1957, Absorption spectra of some silicates in the visible and near infrared: Am. Mineralogist, v. 42, p. 732-742.

Clark, S. P., Jr., Schairer, J. F., and de Neufville, John, 1962, Phase relationship in the system $CaMgSi_2O_6$–$CaAl_2SiO_6$–SiO_2 at low and high pressure: Carnegie Inst. Washington Year Book 61, p. 59-68.

Deer, W. A., Howie, R. A., and Zussman, J., 1962, Rock-forming minerals, v. 1: New York, John Wiley & Sons, 270 p.

DeVries, R. C., Roy, Rustum, and Osborn, E. F., 1956, Phase equilibrium in the system-CaO–TiO_2–SiO_2: Am. Ceramic Soc. Jour., v. 38, p. 158-171.

Eckermann, H. von, 1948, The alkaline district of Alnö Island: Sveriges geol. undersökning, Ser. Ca., v. 36, 176 p.

Erickson, R. L., and Blade, L. V., 1963, Geochemistry and petrology of the alkalic igneous complex at Magnet Cove, Arkansas: U.S. Geol. Survey Prof. Paper 425, 95 p.

Espinosa, G. P. 1964, A crystal chemical study of titanium and chromium substituted yttrium iron and gallium garnets: Inorganic Chemistry, v. 3, p. 848-850.

Geller, S., 1967, Crystal chemistry of the garnets: Zeitschr. Kristallographie, v. 125, p. 1-47.

Geller, S., Miller, C. E., and Treuting, R. G., 1960, New synthetic garnets: Acta Cryst., v. 13, p. 179-186.

Genth, F. A., 1890, Contribution to mineralogy: Am. Jour. Sci., 3d ser., v. 40, p. 114-120.

Gold, D. P., 1966, The minerals of the Oka carbonatite and alkaline complex, Oka, Quebec: Mineralog. Soc. India, IMA v., p. 109-125.

Ito, J., and Frondel, C., 1967, Synthetic zirconium and titanium garnets: Am. Mineralogist, v. 52, p. 773-781.

Gossner, B., 1931, Über die chemische Zusammensetzung in der Granatgruppe: Neues Jahrb., Festband Brauns, v. 64, p. 225-233.

Gossner, B., and Reindl, E., 1934, Über die chemische Zusammensetzung titanhaltiger Silicate insbesondere von Astrophyllit: Zentralbl. Mineralogie, Geologie, und Paläontologie, 1934, Abt. A: Mineralogie Petrographie, p. 161-167.

Hackmann, V., 1900, Neue Mitteilungen über das Ijolithmassiv in Kuusamo: Comm. géol. Finlande Bull., no. 11, p. 1-45.

Huckenholz, H. G., 1968, Oxidation of Ca-rich clinopyroxenes: Carnegie Inst. Washington Year Book 67, in press.

Huckenholz, H. G., Schairer, J. F., and Yoder, H. S., Jr., 1967, Synthesis and stability of ferri-diopside: Carnegie Inst. Washington Year Book 66, p. 334-347.

King, B. C., 1949, The Napak area of southern Karamoja, Uganda: Uganda Geol. Survey Mem. 5, 57 p.

Knop, A., 1877, Uber den Schorlomit von Kaiserstuhl: Zeitschr. Kristallographie Mineralogie, p. 58-64.

König, G. A., 1886, Uber den Schorlomit, eine Varietät des Melanits: Natl. Acad. Sci. Proc., v. 335, p.

Kunitz, W., 1936, Die Rolle des Titans und Zirkoniums in den gesteinsbildenden Silikaten: Neues Jahrb. Mineralogie Geologie, Beil.-Band 70A, p. 385-466.

Kushiro, I., 1960, Si-Al relation in clinopyroxenes from igneous rocks: Am. Jour. Sci., v. 258, p. 548-554.

Larsen, E. S., and Jenks, W. F., 1942, Alkalic rocks of Iron Hill, Gunnison County, Colorado: U.S. Geol. Survey Prof. Paper 197A, p. 1-64.

Majer, V., 1954, Granat aus dem Bache Revkovica in Ostserbien: Zagreb Geol. Bull., v. 5-7, p. 370.

Manning, P. G., 1967, The optical absorption spectra of some andradites and the identification of the $^6A_1 \rightarrow {}^4A_1\ {}^4E(G)$ transition in octahedrally bonded Fe^{3+}: Canadian Jour. Earth Sci., v. 4, p. 1039-1047.

Miyashiro, A., 1959, Notes on rock-forming minerals. (6) Garnet in nepheline-syenite of the Fukushin-Zan district: Geol. Soc. Japan Jour., v. 65, p. 171-172.

Piners., M., 1894, Über Topazolith und Melanit: Zeitschr. Kristallographie Mineralogie, v. 22, p. 479-496.

Sanero, E., 1935, Sopro due granati delle miniere di Cogne in Val d'Aosta: Periodico Min. Roma, v. 6, p. 213.

Seebach, M., 1906, Chemische und mineralogische Studien am Granat: Centralbl. Mineralogie, Geologie, Paläontologie, 1906, p. 774-780.

Shepherd, E. S., and Rankin, G. A., 1909, The binary systems of alumina with silica, lime, and magnesia. With optical study by F. E. Wright: Am. Jour. Sci., 4th ser., v. 28, p. 293-333.

Sobolev, N. Y., 1964, Paragenetic types of garnets: Akad. Nauk SSSR, 1964, 218 p. (in Russian).

Subramanian, A. P., 1956, Mineralogy and petrology of the Sittampundi complex, Salem district, Madras State, India: Geol. Soc. America Bull., v. 67, p. 317-390.

Tarte, P., 1960, Infrared spectra of garnets: Nature, v. 186, p. 234.

Washington, H. S., 1920, Italite, a new leucite rock: Am. Jour. Sci., 4th ser., v. 50, p. 33-47.

Zedlitz, O., 1933, Über titanreichen Kalkeisengranat: Centralbl. Mineralogie, Geologie, Paläontologie, 1933, Abt. A: Mineralogie und Petrographie, p. 225-239.

———— 1935, Über titanhaltige Kalkeisengranate. II: Zentralbl. Mineralogie, Geologie, Paläontologie 1935, Abt. A: Mineralogie und Petrographie, p. 68-78.